Electronic Supplementary Material (ESI) for Nanoscale.

Targeting mechanism for SARS-CoV-2 *in silico:* Interaction and key groups of TMPRSS2 toward four potential drugs

Xiaoyu Zhao,[1] Song Luo,[1] Kaifang Huang,[2] Danyang Xiong,[1] John Z. H. Zhang,[2,3,4] Lili Duan[*,1]*

[1]School of Physics and Electronics, Shandong Normal University, Jinan, 250014, China

[2]Shanghai Engineering Research Center of Molecular Therapeutics and New Drug Development, School of Chemistry and Molecular Engineering, East China Normal University, Shanghai, 200062, China

[3]NYU-ECNU Center for Computational Chemistry at NYU Shanghai, Shanghai, 200062, China

[4]Department of Chemistry, New York University, NY, NY 10003, USA

Corresponding author (duanll@sdnu.edu.cn)

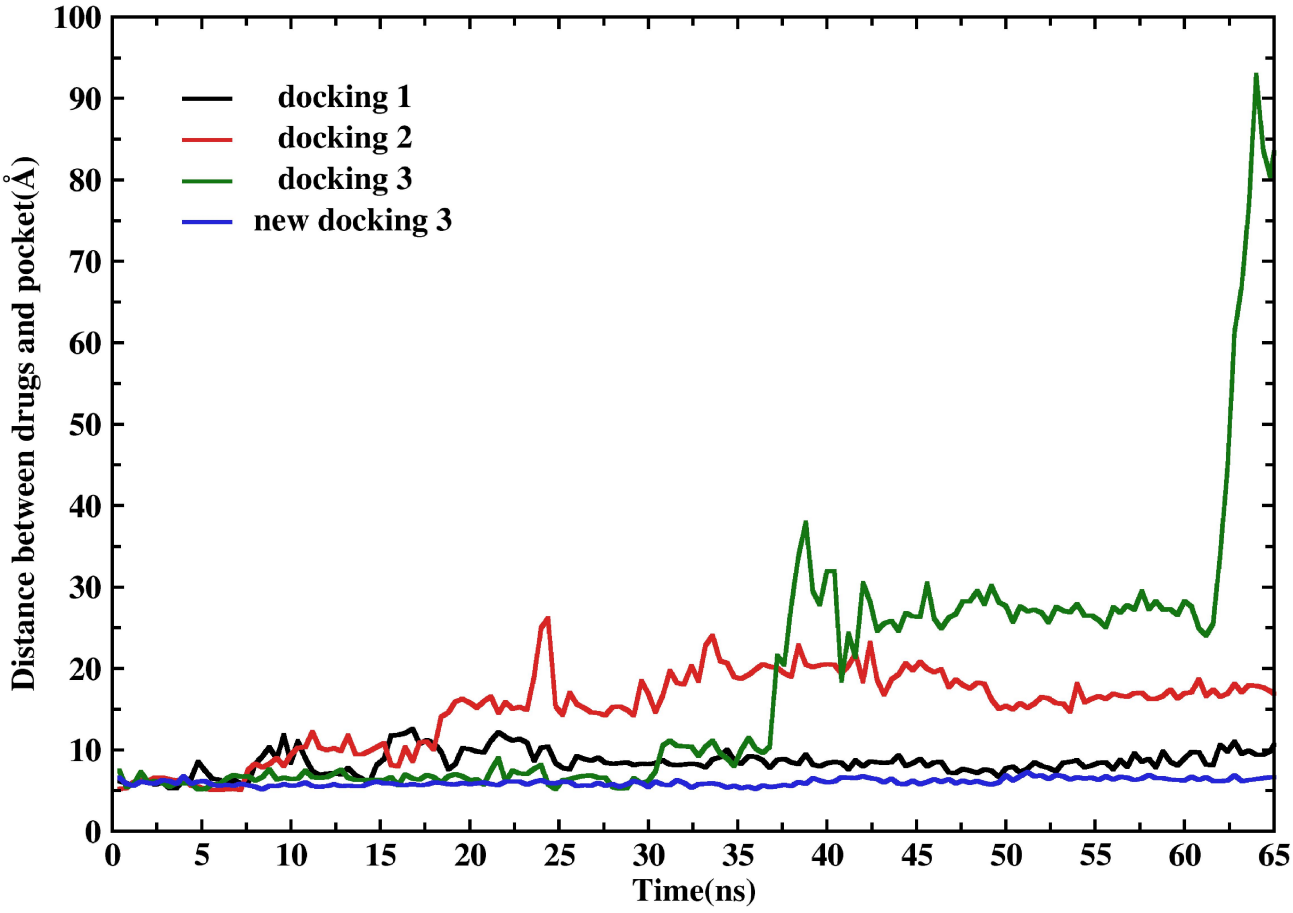

Figure S1. The time evolution of the distance between four docking structures of bromhexine and binding pocket center. Each docking is displayed in a different color.

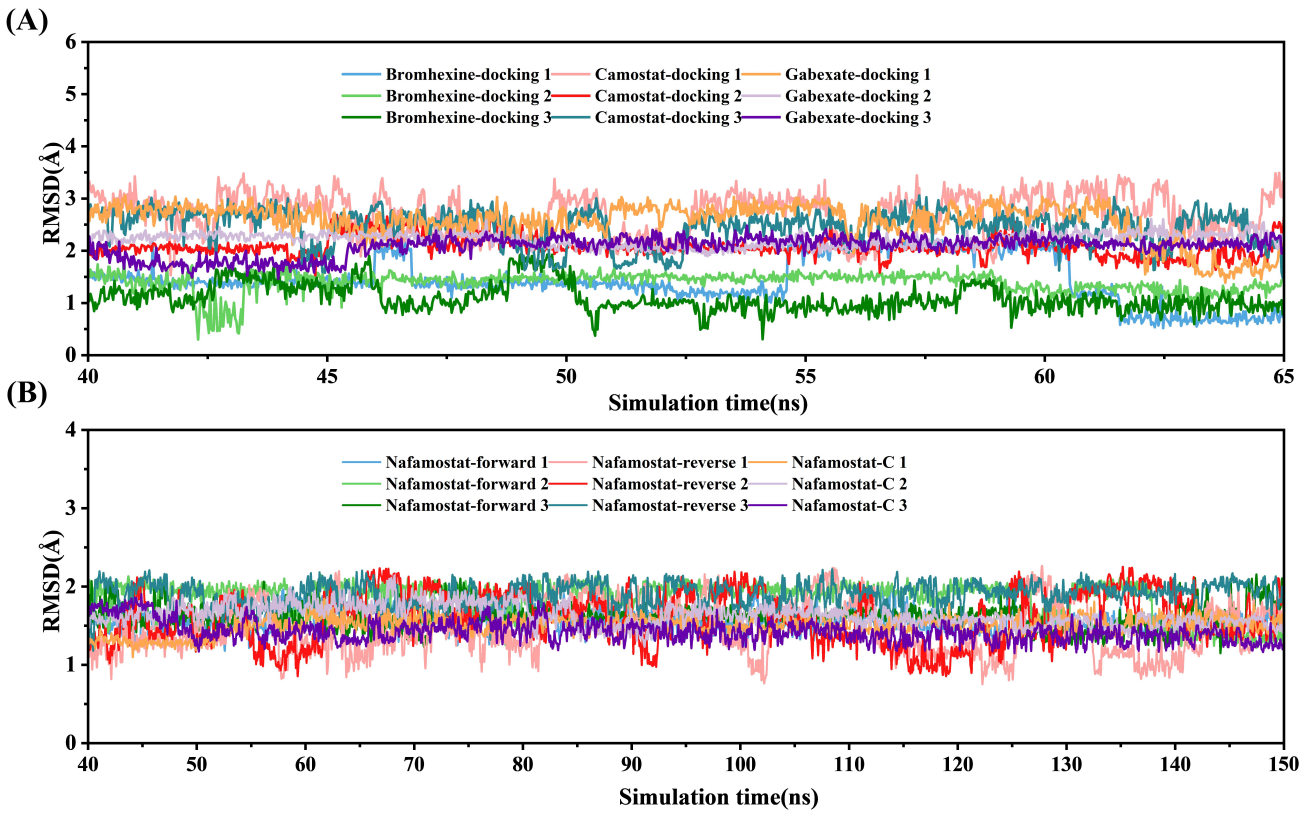

Figure S2. The RMSDs of ligands heavy atoms relative to their initial conformation along MD simulation time.

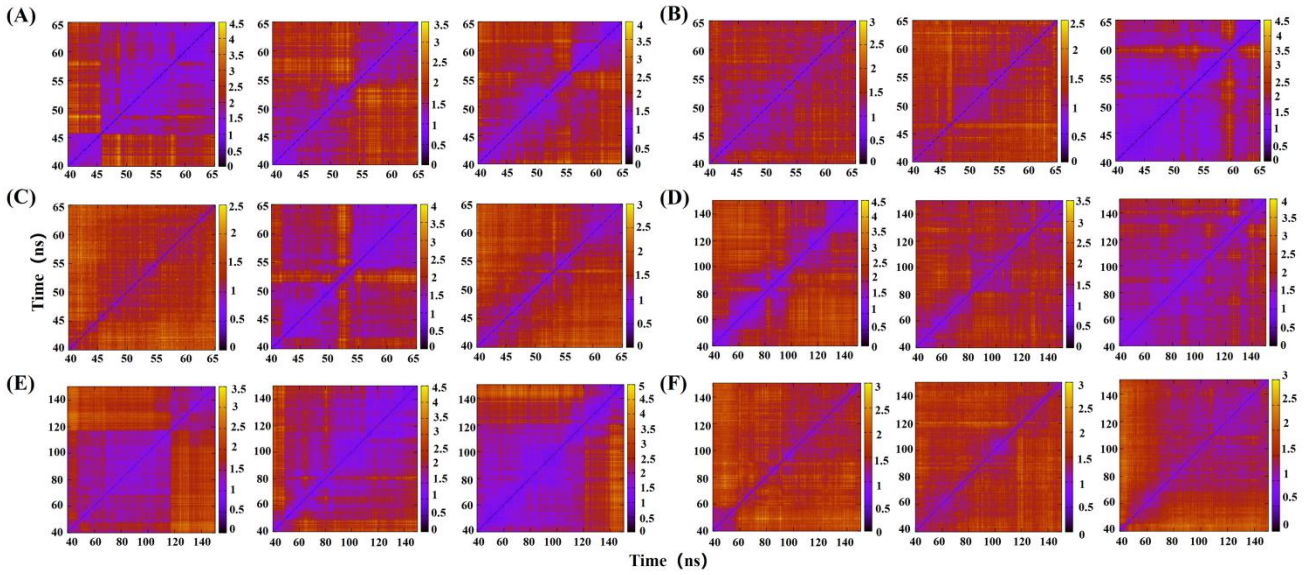

Figure S3. The 2D-RMSD of C_α atoms for (A) the bromhexine–TMPRSS2, (B) the camostat–TMPRSS2, (C) the gabexate–TMPRSS2, (D–F) the three repeat trajectories for each system of nafamostat-forward, nafamostat-reverse, and nafamostat-C, respectively.

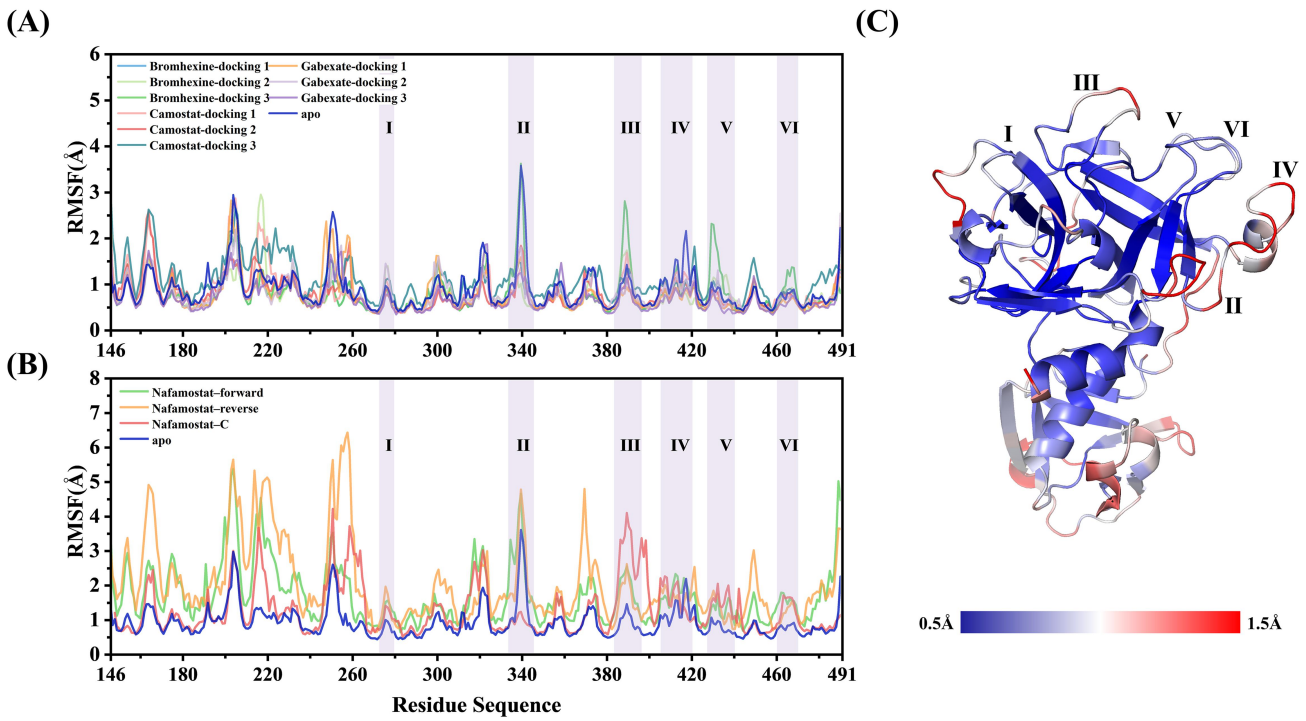

Figure S4. The RMSF for (A) bromhexine, camostat, gabexate, (B) nafamostat-forward/reverse/C, and apo state is evaluated as a comparison, of which six regions are marked with light purple shading. The apo state curve is markedly colored for contrast, and RMSF mapping of the apo protein is displayed on (C), in which six regions are marked.

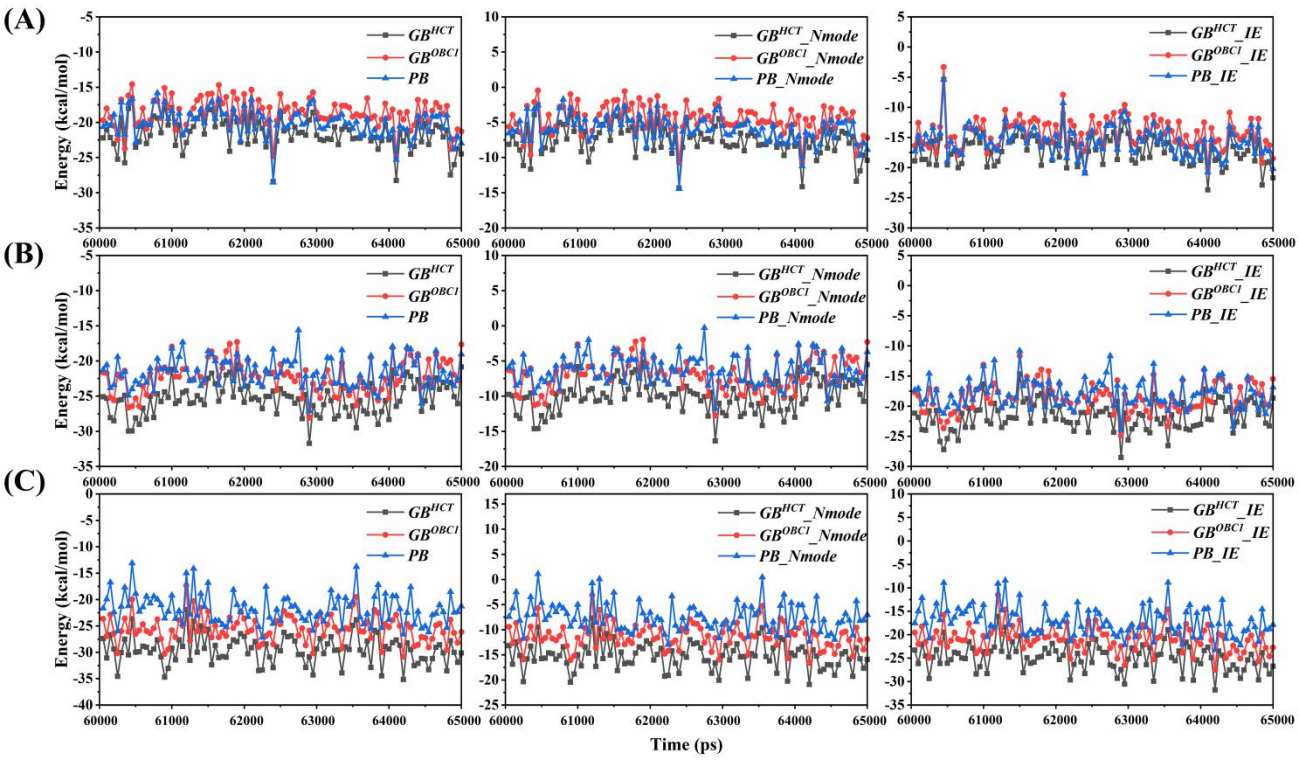

Figure S5. The fluctuations of the binding free energies for the bromhexine bound TMPRSS2 complexes in nine methods. (A), (B), and (C) show the MD simulation results of three docking structures, respectively.

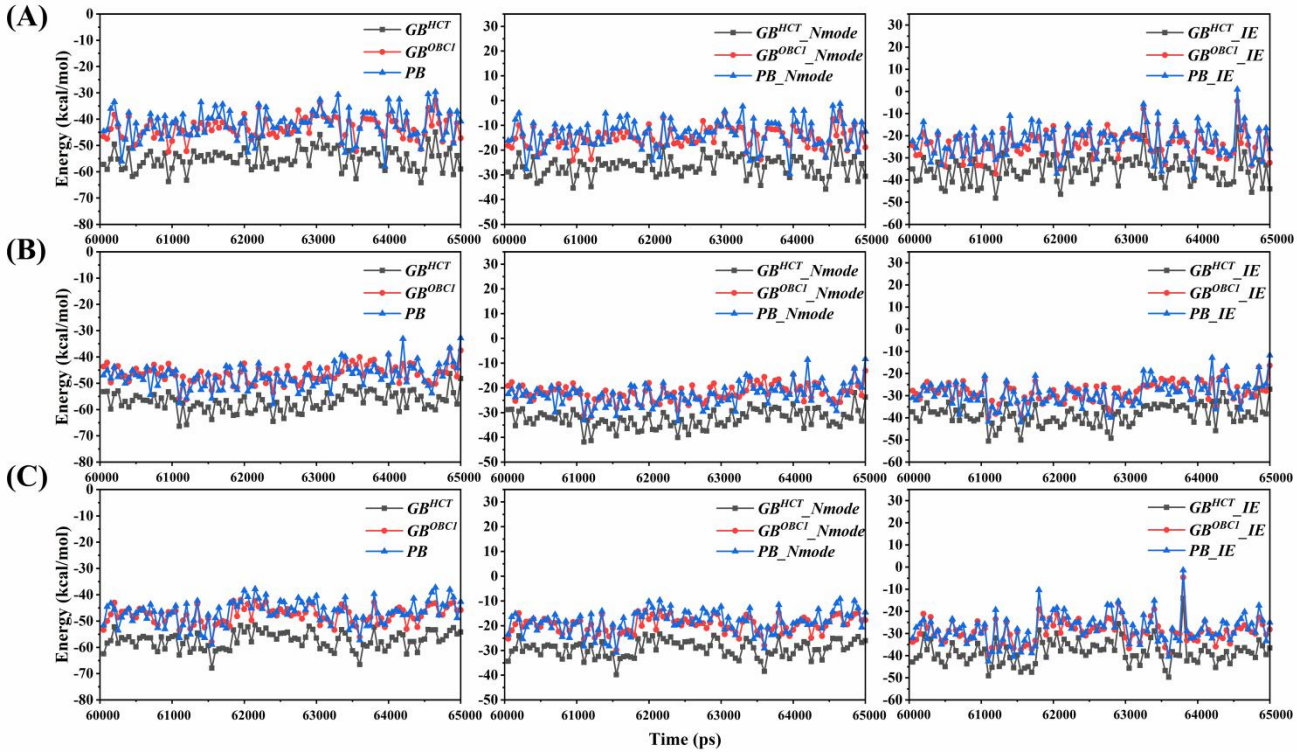

Figure S6. The fluctuations of the binding free energies for the camostat bound TMPRSS2 complexes in nine methods. (A), (B), and (C) show the MD simulation results of three docking structures, respectively.

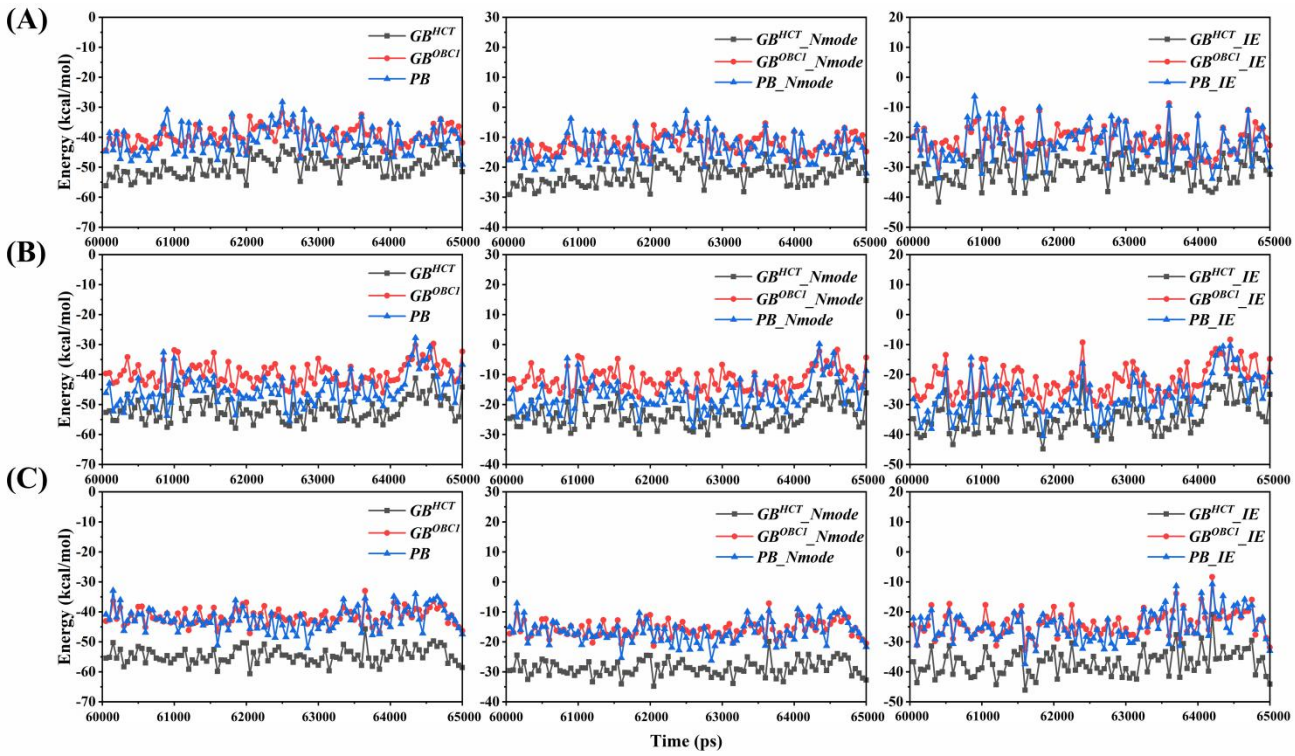

Figure S7. The fluctuations of the binding free energies for the gabexate bound TMPRSS2 complexes in nine methods. (A), (B), and (C) show the MD simulation results of three docking structures, respectively.

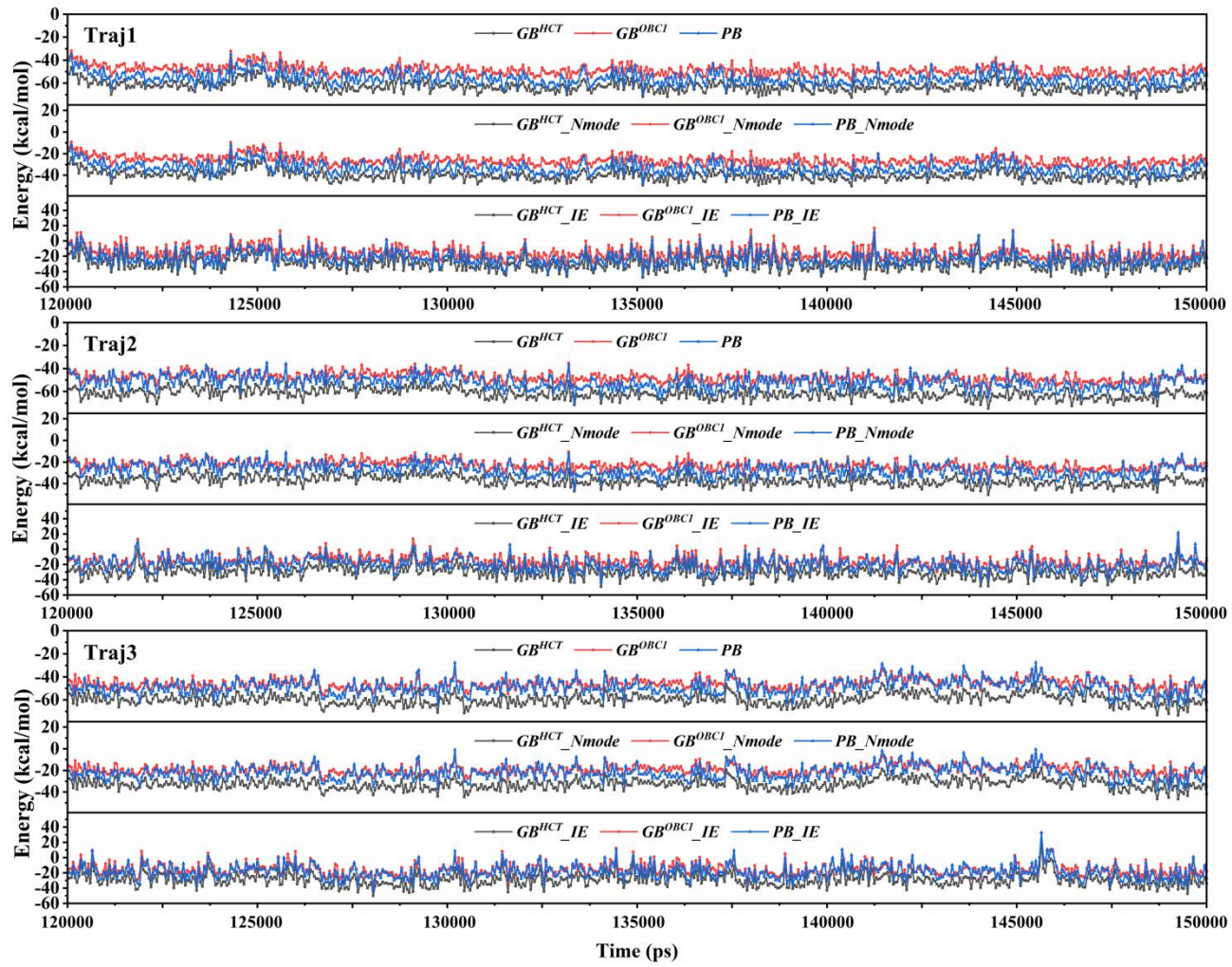

Figure S8. The fluctuations of the binding free energies for the nafamostat-forward bound TMPRSS2 complexes in nine methods. The results of three repeated MD simulations are shown, respectively.

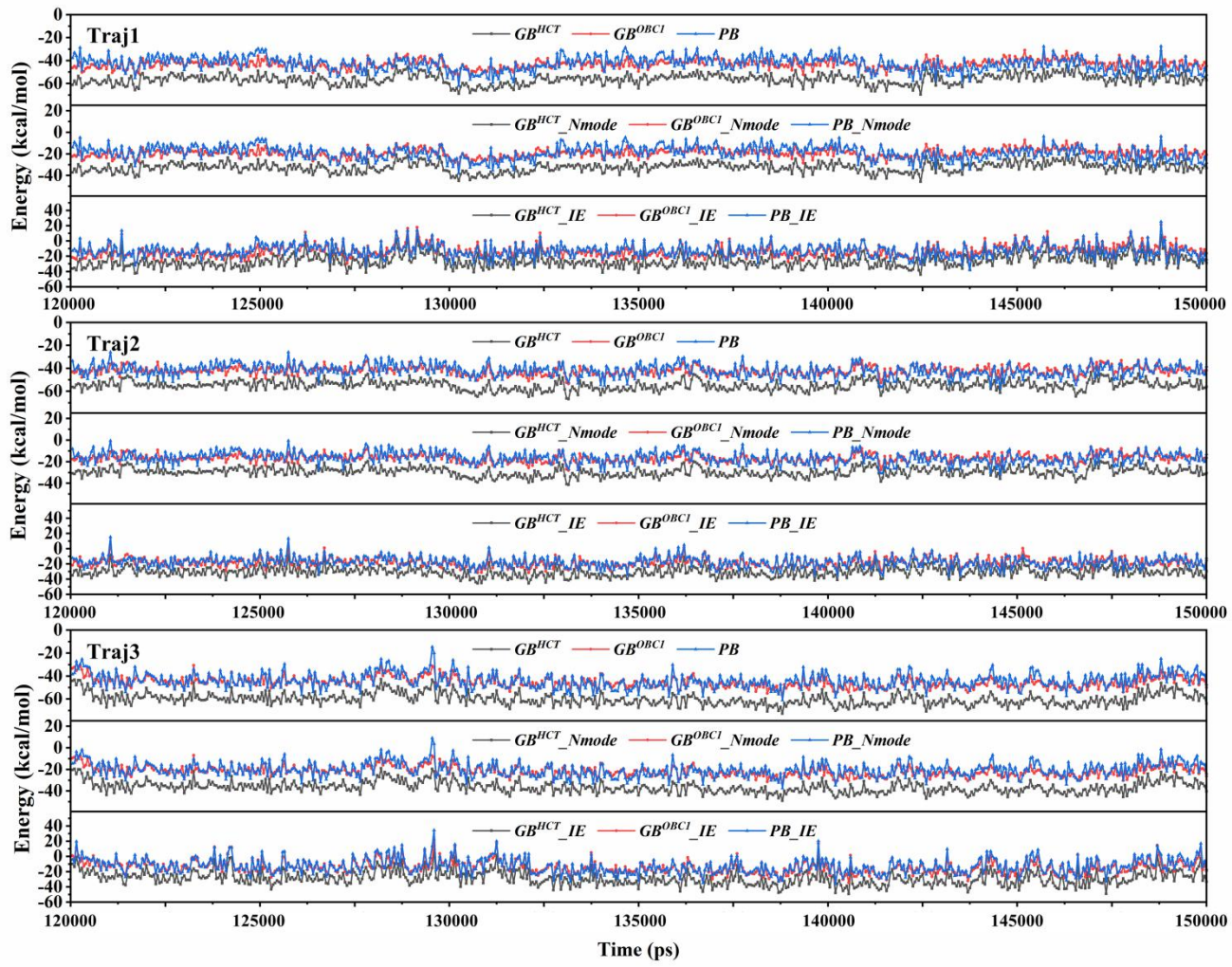

Figure S9. The fluctuations of the binding free energies for the nafamostat-reverse bound TMPRSS2 complexes in nine methods. The results of three repeated MD simulations are shown, respectively.

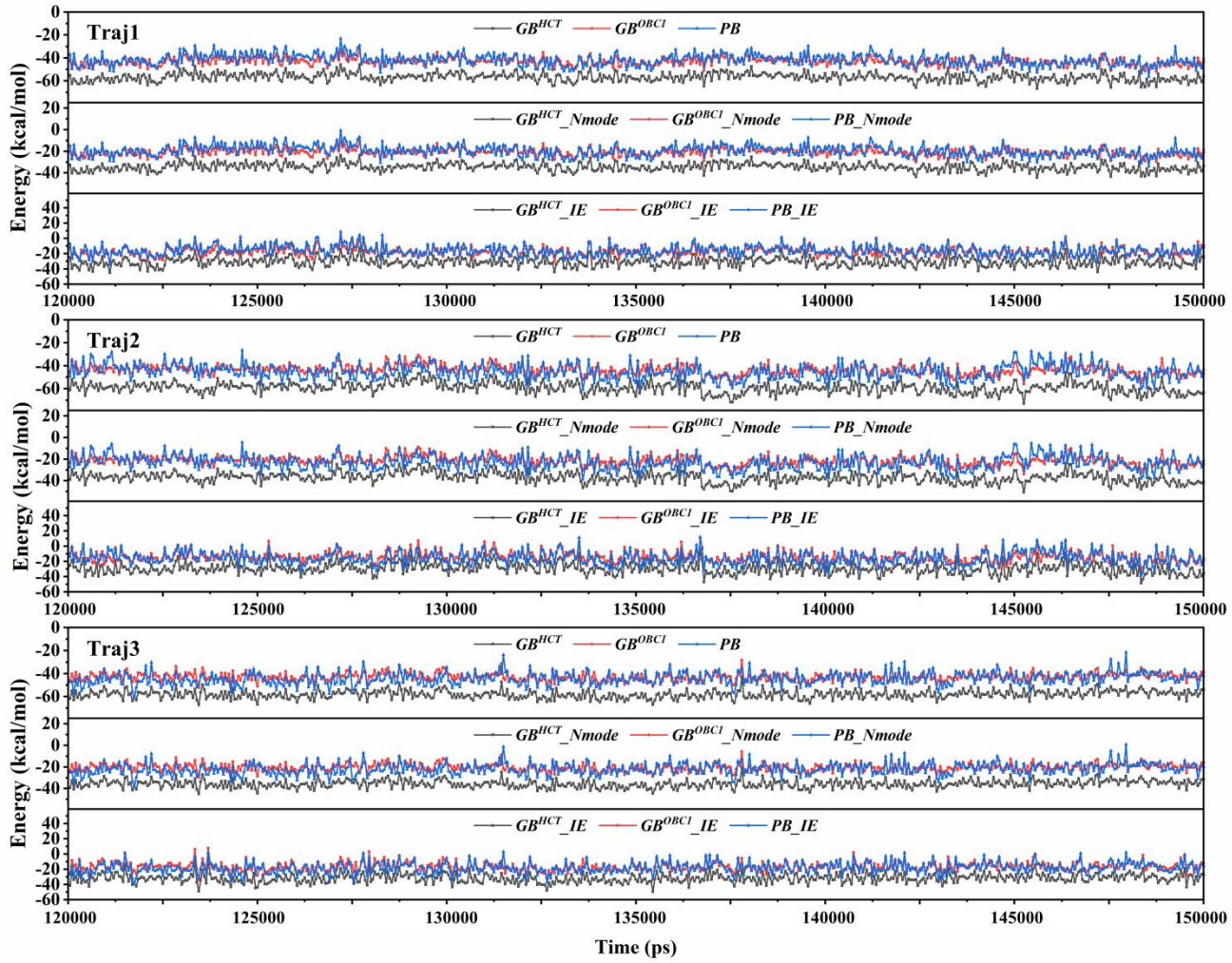

Figure S10. The fluctuations of the binding free energies for the nafamostat-C bound TMPRSS2 complexes in nine methods. The results of three repeated MD simulations are shown, respectively.

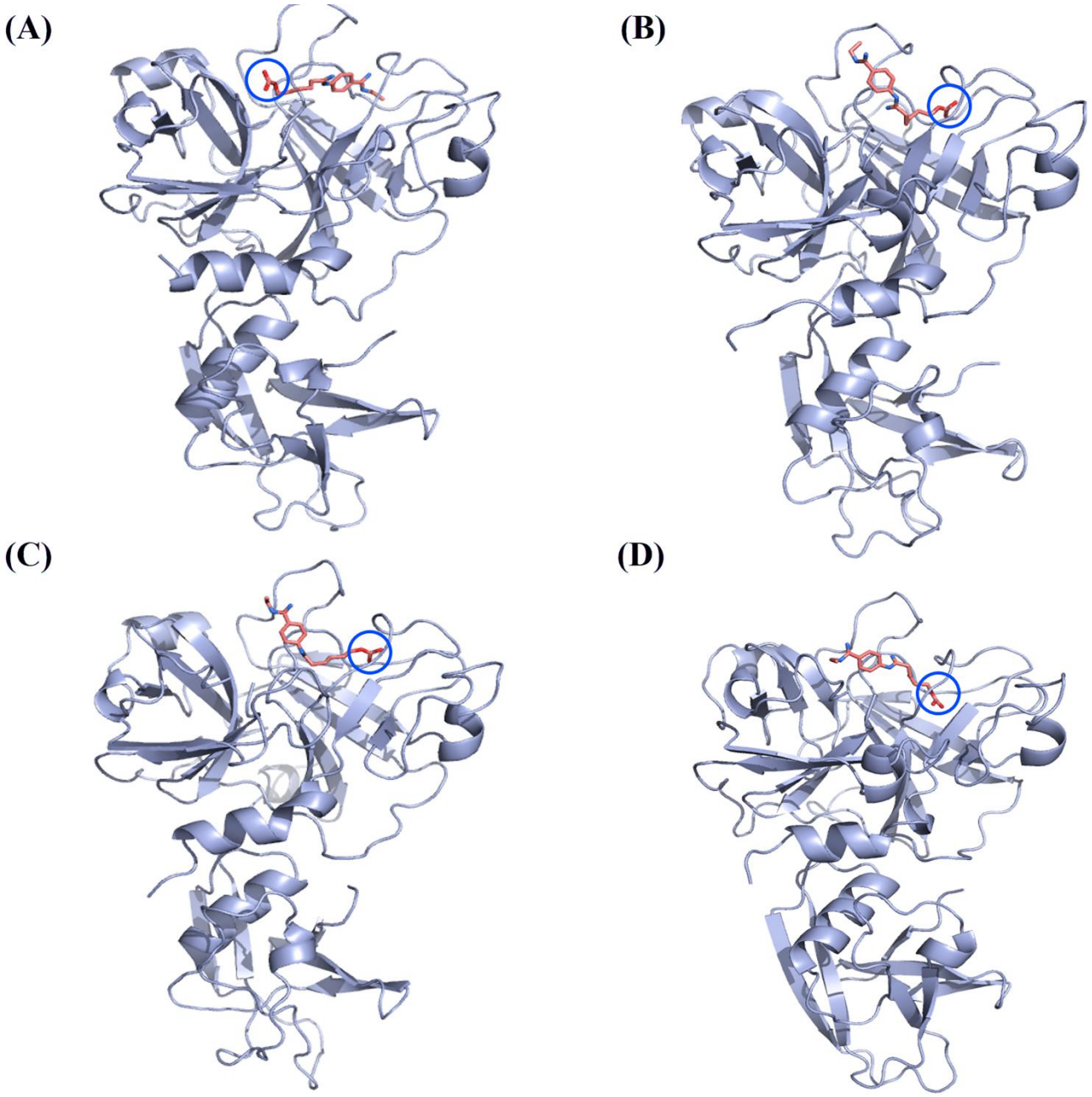

Figure S11. The representative conformations of the four docking structures for gabexate, where the blue circles are labeled the guanidinium group, (A) original docking 1, (B) docking 1, (C) docking 2, and (D) docking 3.

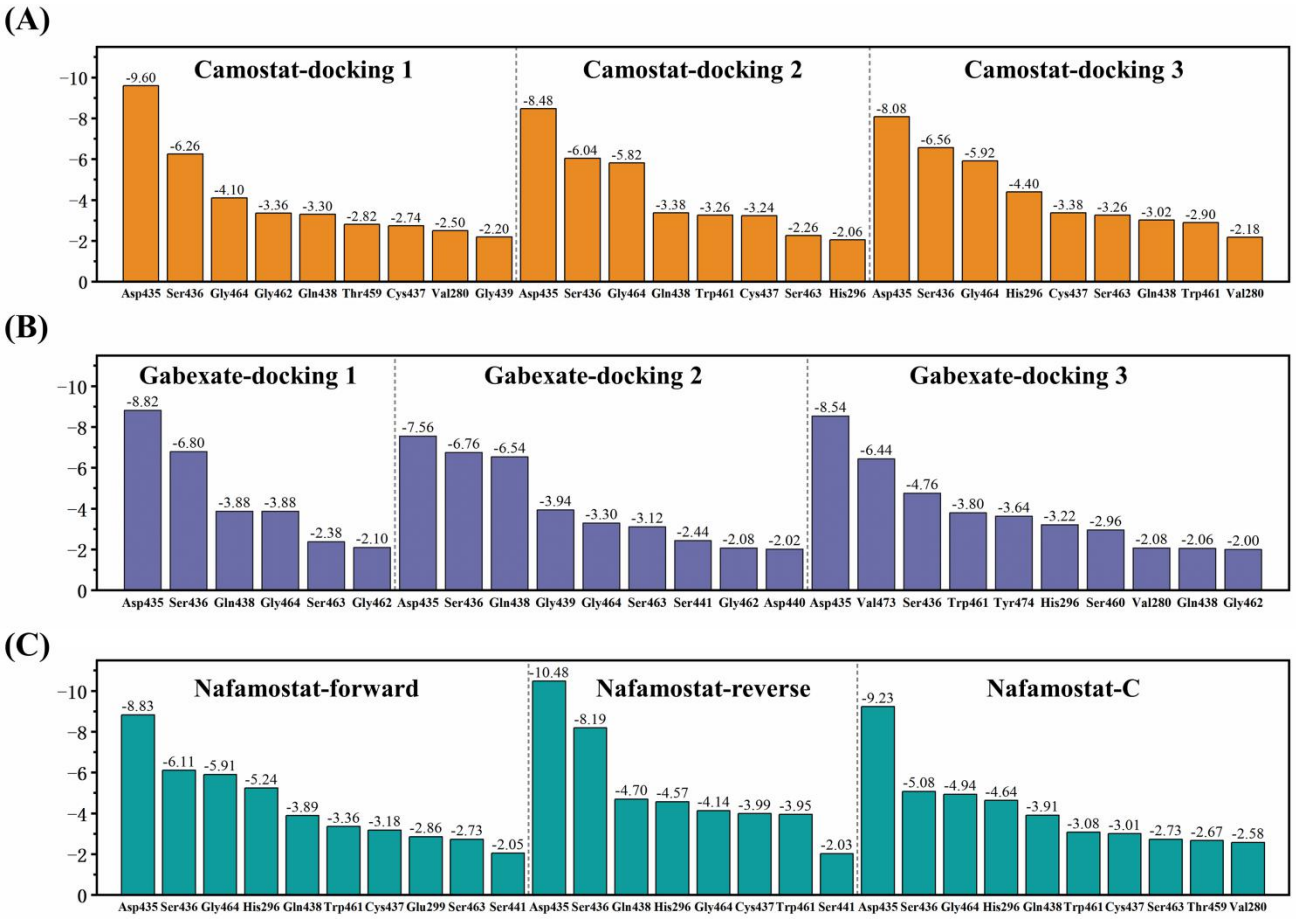

Figure S12. The energy contributions of hot-spot residues for each docking structure in (A) camostat–TMPRSS2 and (B) gabexate–TMPRSS2, and (C) nafamostat–TMPRSS2. All values are in kcal/mol.

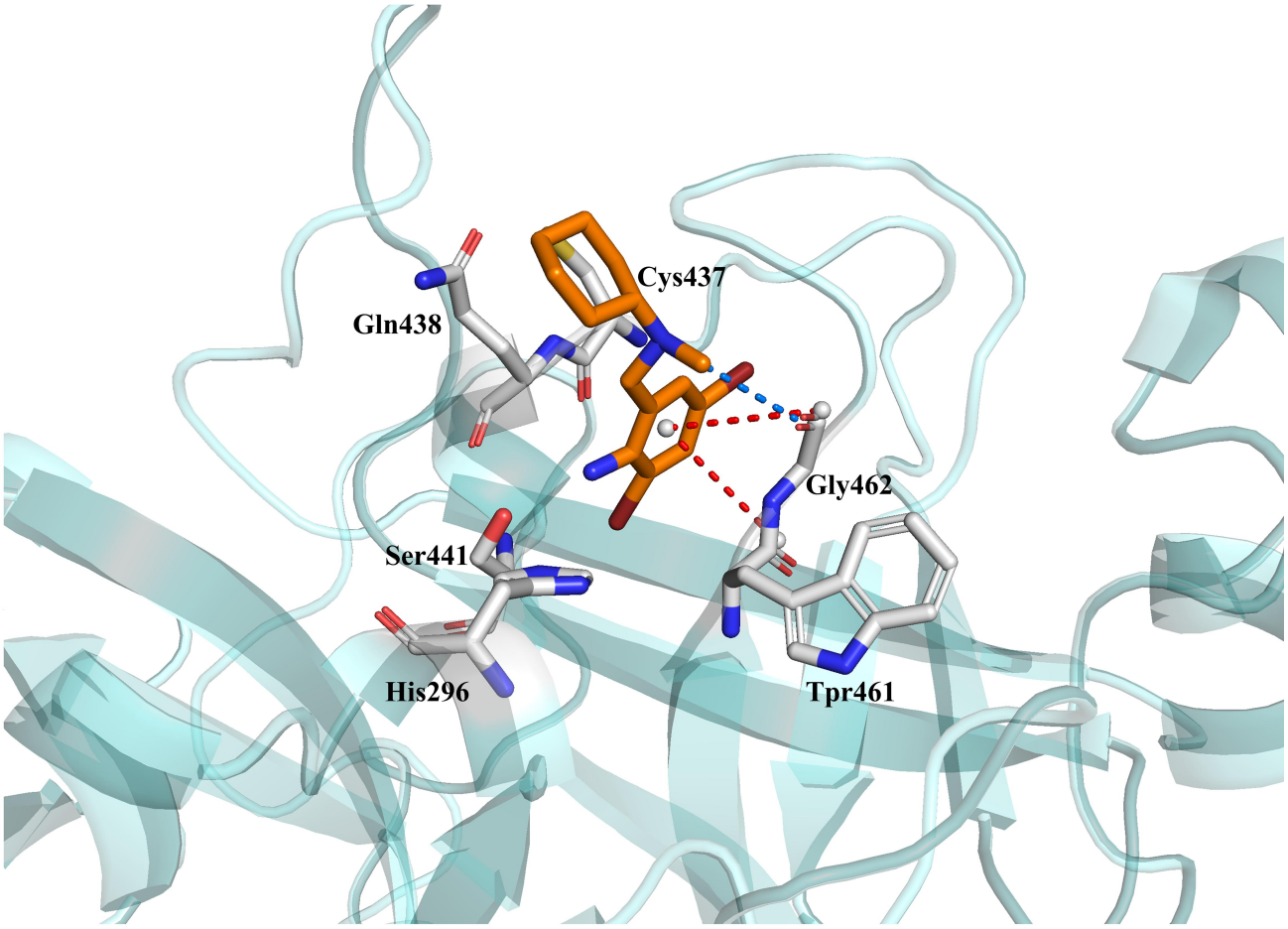

Figure S13. The interaction mode between hot-spots and the representative structures of bromhexine.

CH–O interaction (blue), π–Amide interactions (red), all values are in Å.

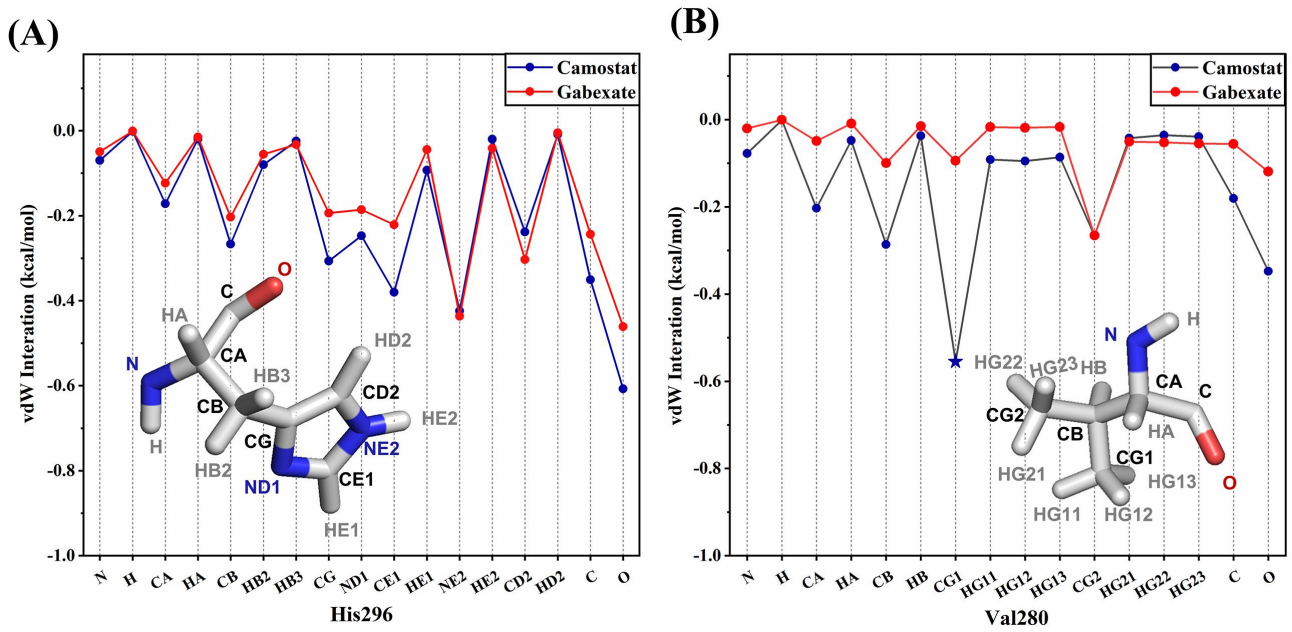

Figure S14. The vdW interaction of per atom with camostat or gabexate in (A) His296 and (B) Val280 residues.

Table S1. The enthalpy terms in the binding free energy for each docking structure of three drugs to TMPRSS2 calculated by GB^{HCT}, GB^{OBC1}, GB^{OBC2}, GB^{GBn1}, and PB models, respectively. All values are in kcal/mol.

Drugs	System	GB^{HCT}	GB^{OBC1}	GB^{OBC2}	GB^{GBn1}	PB
Bromhexine	Docking 1	-21.58±0.22	-18.67±0.21	-36.88±0.62	-38.41±1.04	-20.14±0.20
	Docking 2	-25.46±0.22	-22.21±0.23	-38.02±0.63	-44.03±0.60	-21.73±0.21
	Docking 3	-29.50±0.26	-25.50±0.25	-38.33±0.58	-31.69±1.00	-21.77±0.29
Camostat	Docking 1	-55.05±0.39	-43.36±0.40	-20.53±0.86	-5.58±1.69	-41.90±0.57
	Docking 2	-56.99±0.36	-46.44±0.35	-25.67±0.91	-9.84±1.41	-47.18±0.53
	Docking 3	-57.37±0.33	-47.73±0.33	-29.40±0.90	-8.60±2.00	-46.54±0.46
Gabexate	Docking 1	-49.68±0.33	-39.49±0.32	-3.38±0.78	19.75±1.40	-40.81±0.45
	Docking 2	-51.66±0.38	-39.71±0.37	-4.75±0.85	14.00±1.92	-44.96±0.53
	Docking 3	-54.54±0.26	-41.56±0.27	8.45±1.03	5.40±2.24	-42.35±0.38
Nafamostat-forward	Trajectory 1	-62.83±0.45	-48.64±0.42	-20.66±0.97	6.46±1.90	-55.84±0.55
	Trajectory 2	-61.88±0.45	-47.78±0.41	-14.99±0.94	24.23±1.37	-52.03±0.59
	Trajectory 3	-59.63±0.48	-46.12±0.43	-16.55±0.94	15.26±1.57	-48.90±0.63
	Average	-61.45±0.48	-47.51±0.43	-17.40±0.98	15.31±1.78	-52.26±0.66
Nafamostat-reverse	Trajectory 1	-56.45±0.45	-43.20±0.38	-11.75±1.02	21.80±1.58	-42.85±0.62
	Trajectory 2	-54.88±0.40	-42.18±0.36	-10.82±0.81	19.34±1.52	-41.81±0.53
	Trajectory 3	-60.17±0.51	-45.43±0.46	-18.85±0.92	27.28±1.47	-43.93±0.65
	Average	-57.17±0.51	-43.61±0.42	-13.81±0.99	22.81±1.56	-42.86±0.61
Nafamostat-C	Trajectory 1	-56.86±0.35	-43.24±0.38	-8.06±0.96	38.09±1.58	-41.82±0.48
	Trajectory 2	-59.28±0.47	-43.66±0.43	2.04±1.29	46.52±1.77	-45.15±0.65
	Trajectory 3	-58.25±0.34	-42.88±0.35	12.29±1.12	66.57±1.64	-44.38±0.52
	Average	-58.13±0.40	-43.26±0.37	2.09±1.40	50.39±2.04	-43.78±0.57

Table S2. The energy terms of the three repeated MD trajectories for nafamostat–TMPRSS2 systems, in which the entropy term is obtained by interaction entropy (IE) and Normal mode (Nmode) methods. All values are in kcal/mol.

Structure	Trajectory	ΔE_{ele}	ΔE_{vdW}	ΔG_{gb}^{HCT}	ΔG_{SA}^{HCT}	ΔG_{gb}^{OBC1}	ΔG_{SA}^{OBC1}	ΔG_{pb}^{PB}	ΔG_{SA}^{PB}	*Nmode*	*IE*
Nafamostat-forward	1	-167.57	-41.67	151.70	-5.29	164.28	-3.67	158.31	-4.89	22.61	33.08
	2	-149.72	-38.33	131.41	-5.24	143.91	-3.64	140.88	-4.87	24.64	32.13
	3	-153.18	-38.33	137.34	-5.21	149.26	-3.62	147.71	-4.84	26.92	30.59
Nafamostat-reverse	1	-141.33	-36.53	126.63	-5.21	138.28	-3.62	139.86	-4.84	23.85	29.77
	2	-109.33	-36.44	95.91	-5.02	107.08	-3.48	108.66	-4.70	25.38	24.24
	3	-130.93	-35.11	111.15	-5.28	124.28	-3.67	127.00	-4.89	23.71	31.29
Nafamostat-C	1	-95.60	-41.79	86.29	-5.75	98.14	-3.99	100.83	-5.25	22.19	25.70
	2	-122.29	-44.46	113.38	-5.91	127.20	-4.10	126.97	-5.37	22.21	29.58
	3	-109.44	-42.90	99.80	-5.71	113.43	-3.97	113.18	-5.22	22.43	26.24

Table S3. The binding free energy for the original docking 1 of gabexate calculated by nine methods. Trajectories 1, 2, 3 represent fist 65 ns MD simulation, repeated 65ns MD simulation, and extended 150 ns MD simulation, respectively. All values are in kcal/mol.

Trajectory	GB^{HCT}	GB^{OBC1}	PB	GB^{HCT}_Nmode	GB^{HCT}_IE	GB^{OBC1}_Nmode	GB^{OBC1}_IE	PB_Nmode	PB_IE
1	-40.01±0.53	-31.63±0.42	-27.48±0.55	-16.49±0.99	-16.03±0.53	-8.11±0.94	-7.65±0.42	-3.96±1.00	--3.50±0.55
2	-41.41±0.48	-33.37±0.42	-24.60±0.57	-18.02±1.41	-19.86±0.48	-9.98±1.39	-11.82±0.42	-1.21±1.45	-3.05±0.57
3	-30.35±0.51	-23.14±0.44	-19.76±0.54	-7.17±0.86	-11.09±0.51	-0.04±0.82	-3.88±0.44	3.42±0.88	-0.51±0.54